Eur Biophys J (1988) 15: 293–298

European Biophysics Journal

Loosening of the phage structure in a low ionic strength environment

Gy. Rontó * [1], K. Tóth [1], G. Csik [1], L. A. Feigin [2], D. T. Svergun [2], A. T. Dembo [2], and E. V. Shtikova [3]

[1] Institute of Biophysics, Semmelweis Medical University, P.O.B. 263, H-1444 Budapest, Hungary
[2] Institute of Crystallography, Academy of Sciences of the USSR, Leninsky prospect 59, SU-117333 Moscow, USSR
[3] Institute of Haematology and Blood Transfusion, Nov Zykovsky prospect 4a, SU-125167 Moscow, USSR

Received Decembre 12, 1986/Accepted in revised form August 6, 1987

Abstract. Structural parameters of phage T7 were compared in two frequently used *Tris* buffers of high and low ionic strength, in order to explain the different biological activity and drug-binding characteristics.

Characteristics of the whole phage geometry were obtained by viscosimetry, static and quasi-elastic light-scattering and small-angle X-ray scattering. The latter method revealed dissimilarities in the intraphage DNA compactness, consistent with the findings of the optical absorption melting studies.

Alterations in the particle dimensions determined in the same sample by different methods are discussed, and a model is constructed to explain the structural modifications that occur on lowering the ionic strength.

Key words: Nucleoprotein structure, small-angle X-ray scattering, light-scattering

Introduction

For the last ten years peculiarities of nucleoprotein conformation connected with its biological state have revealed the importance of structural investigations. Difficulties arise from the fact that quite different sample preparations are often needed for structural and biological studies. This means that from the large number of factors influencing the structure, only a few can be kept constant. One of these factors is the ionic environment; its variation can produce conformational changes of macromolecules in solution (e.g. Ausio et al. 1984) and can be important in cells. This factor can also alter the degree of binding of drugs and enzymes to nucleic acids (Lohman et al. 1978).

Our purpose was to study the effect of monovalent salt concentration on the structure and function of a single nucleoprotein complex, i.e. bacteriophage T7. This phage was selected because considerable structural and biological data is already available (e.g.: Studier 1972; Serwer 1976). Recently, phage T7 was also found to be a good candidate for genetic engineering, as its RNA polymerase seems to be efficient at transcribing almost any DNA linked to a promoter (Studier and Moffett 1986). This type of nucleoprotein also represents a model for chromosomes (Rontó 1984). Salt-dependent conformational changes of isolated DNA are well established (Schellman et al. 1984). The sensitivity of DNA to UV-inactivations is also dependent on ionic conditions (Larcom et al. 1981) and the dependence of the chromatin size on salt concentration has been reported (Ausio et al. 1984). Thermal denaturation and biological activity as functions of mono- and bivalent ion concentrations for the same T7 samples were presented in our previous work (Tóth et. al. 1987). In this paper the methods of optical melting, fluorimetry, viscosimetry, static and dynamic light-scattering and small-angle X-ray scattering are applied to study the structure of phage T7 in two different salt environments. Their comparison made it possible to build up a model of conformational changes leading to the biological alterations.

Materials and methods

T7 phages were grown on Escherichia coli B host cells. The cultivation was carried out according to the method described by Gáspár et al. (1980). For the physical and chemical measurements the samples were purified and concentrated as described by Strauss and Sinsheimer (1963). Phages were separated on CsCl gradients and gradually dialysed against the required buffer.

Buffer H (high ionic strength) contains 100 mmol · l^{-1} NaCl and 40 mmol · l^{-1} *Tris*-HCl; buffer L (low ionic strength) – 10 mmol · l^{-1} NaCl and 10 mmol · l^{-1} *Tris*-HCl, both adjusted to pH = 7. Buffer M9 used as a reference in the biological measure-

* To whom offprint requests should be sent

ments contains 20 mmol · l^{-1} NH_4Cl, 40 mmol · l^{-1} Na_2HPO_4, 20 mmol · l^{-1} KH_2PO_4 and 1 mmol · l^{-1} $MgSO_4$. Phage concentrations were determined by optical density at 260 nm. The concentration 0.06 mg/ml was used for viscosity studies, 0.05–0.10 mg/ml for optical measurements, 4–90 mg/ml for X-ray scattering.

Biological activity of the phages was tested by plaque-forming ability measurements taking samples after 2, 30, 60, 90 and 120 min of incubation. Survival rates N/N_0 have been determined where N and N_0 are the number of active phages in the buffer used and in the reference buffer M 9, respectively.

Fluorescence spectroscopy was used to measure the binding affinity of 4'-aminomethyl-4,5',8-trimethylpsoralen (AMT) to the phage. The excitation wavelength was 340 nm, and emission was detected at 450 nm on a Jobin-Yvon mark 3 spectrofluorimeter. The complex-formation was calculated from the measured intensities:

$$(I_0 - I)/I = [\mathrm{AMT}_{\mathrm{complexed}}]/[\mathrm{AMT}_{\mathrm{free}}], \quad (1)$$

where I_0 and I are the emitted intensities for the drug in the absence and presence of the phage T 7, respectively.

Viscosity measurements were carried out on a Ubbelohde capillary viscosimeter. Reduced viscosities were calculated as

$$\eta_{\mathrm{red}} = (t/t_0 - 1)/c, \quad (2)$$

where c is the phage concentration of the sample, t and t_0 – flowing times for the solution and the solvent, respectively.

Melting studies were done by optical absorption at 260 nm using a Perkin-Elmer 200 UV-VIS spectrophotometer. The heating rate was 0.5 °C/min. Data sets were collected by an on-line coupled computer to calculate the first derivative and its momenta.

Static light-scattering (SLS). The angular distribution of the scattered light was detected from 30° to 150° using an Argon-ion laser (488.8 nm) and an ALV detection system. The radius (R_L) of the phage particle was calculated through a spherical approximation, using the dissymetry factor at $\Theta = 45°$ and 135° (Kerker 1969).

Quasi-elastic light-scattering (*QELS*) measurements were done on a Malvern 4200 spectrometer at a wavelength of 632.8 nm. Translational diffusion coefficients, D_t, were determined by one-exponential fitting (Cummings and Pike 1974). The Stokes radii, R_H, were calculated using the relation

$$R_H = kT/(6\pi\eta D_t), \quad (3)$$

where η is the viscosity of the solvent.

Small-angle X-ray scattering (SAXS) studies were performed with automatic SAXS diffractometers. A wavelength of 0.154 nm was used, and the scattering intensity, $I(s)$, was determined using the function

$$s = 4\pi \sin\theta/\lambda, \quad (4)$$

where 2θ is the scattering angle.

The initial parts of the curves from $s = 0.01\ \mathrm{nm}^{-1}$ up to $0.35\ \mathrm{nm}^{-1}$ were measured on a Kratky camera at different concentrations and extrapolated to zero concentration. Outer parts ($0.2 < s < 4.5\ \mathrm{nm}^{-1}$) were measured on the diffractometer with a position-sensitive detector (Mogilevsky et al. 1984). The data sets were smoothed and desmeared as described (Schedrin and Feigin 1966, Rolbin et al. 1980). Particle radius of gyration, R_g, was calculated from the Guinier formula (Glatter and Krattky 1982)

$$I(s) = I(0) \cdot \exp(-s^2 R_g^2/3). \quad (5)$$

The Porod volume (V) can be evaluated from the equation

$$V = 2\pi^2 I(0)/\int_0^\infty s^2 I(s)\,\mathrm{d}s \quad (6)$$

In Eqs. (5) and (6) $I(s)$ denotes the scattered intensity at the corresponding s values defined by Eq. (4). The distance distribution function $p(r)$, a spherically averaged self-convolution of the particle excess electron density (Glatter and Kratky 1982), is connected to the scattering intensity by the transformation

$$p(r) = r^2/(2\pi^2) \int_0^\infty s^2 I(s)(\sin sr/sr)\,\mathrm{d}s \quad (7)$$

while the radial density distribution of $\varrho(r)$ for a spherically-symmetric particle can be calculated as

$$\varrho(r) = 1/(2\pi^2) \int_0^\infty [\pm\sqrt{I(s)}]s^2(\sin sr/sr)\,\mathrm{d}s. \quad (8)$$

Hence the signs of the scattering amplitudes can be determined by the iterative procedure of Svergun et al. (1984).

Results and discussion

Figure 1 shows the effect of incubation in buffers L and H on the biological activity. It is evident that a high degree of inactivation takes place in buffer L after only a few minutes of incubation. At the same time, the phage in buffer H remains almost completely active after several hours of incubation. Moreover, fluorescent binding studies of an intercalating drug AMT show 5 times higher dark-binding activity in buffer L than in buffer H.

These data suggest that the structure of phage T 7 may be different in buffer L and H. In order to investigate the structure of phages in buffers H and L several physico-chemical methods were applied, these are suitable for detecting different structural charac-

Table 1. Characteristic data of phage T7 in buffers H and L

Methods used	Biological activity N/N_0 [1]	Viscosity η reduced	Optical melting (OD_{260})		SLS	QELS	SAXS		
			T_1	$T_{2(b)}$	R_L	$R_H^{(2)}$	R_g	V	$R_{g(\text{head})}$
Buffers		(dl/g)	°C	°C	(nm)	(nm)	(nm)	(nm^3)	(nm)
H	0.95	0.07	55.2	89.2	40	29	25.8	1.14×10^5	23.6
L	0.15	0.72	55.0	76.5	62	54	25.3	0.91×10^5	24.8
Accuracy	± 0.05	± 0.02	± 0.5	± 0.2	± 2	± 2	± 0.3	± 0.1 $\times 10^5$	± 0.3

[1] after one hour of incubation
[2] with no account of rotational diffusion

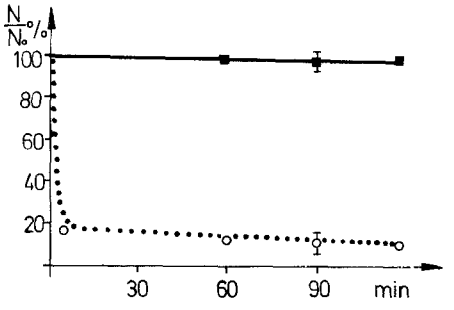

Fig. 1. Biological inactivation of phage T7. Survival ratios of phage T7 in buffers H (——) and L (....) with respect to the phosphate buffer M9 as a function of the incubation time

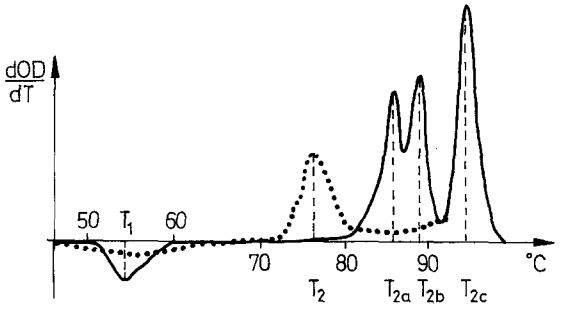

Fig. 2. Derivative melting curves of phage T7 measured by optical absorption at 260 nm in buffer H (——) and L (....) as a function of the temperature. Melting temperatures are determined as first momenta of the curves

teristics. Table 1 summarizes the results of these studies, including the biological activities (survival ratios). The accuracies of each method are also indicated.

Reduced viscosities of the phage T7 solutions prove to be 0.07 and 0.72 dl/g for H and L buffers, respectively. One can see that this parameter changes drastically, as survival ratios change, but remains smaller than for free phage DNA in solution (its value, 16 dl/g, was obtained for the samples heated to 65 °C and was the same for buffers L and H).

Figure 2 presents the optical absorption melting studies of phage nucleoprotein at 260 nm in the two buffers. The two curves show many dissimilarities which represent the differences in the heat stability of the phage.

The low temperature range (T_1, see Fig. 2) refers to phage disruption (Fekete et al. 1982). One can observe that this temperature remains unchanged in buffer L, but there is a broadening at the peak. It suggests that the process of phage disruption is somewhat smeared in this case. In the higher temperature range there are three peaks (*a*, *b*, *c*) of the derivative melting curve in buffer H. The peak at $T_{2b} = 89.2\,^\circ$ corresponds to DNA melting, i.e. H-bond breaking (Tóth and Rontó 1987). For buffer L only a single broad peak is found at the temperature $T_2 = 76.5\,^\circ$C, which is also associated with H-bond breaking. The more than 10 °C decrease of the DNA melting temperature indicates that the stability of the phage DNA is lower in the case of buffer L.

Light-scattering methods were used to estimate the dimensions of the phage particles. The particle radii R_L as determined by SLS prove to be 40 and 62 nm for buffers H and L, respectively. QELS measurements allowed us to obtain translational diffusion coefficients of the phage which proved to be 7.50×10^{-8} and 4.00×10^{-8} cm^2/s in the H and L buffers. With these values the Stokes radii R_H were estimated, they proved to be 29 and 54 nm for the H and L buffers.

The absolute values of the phage dimensions are different for the two methods even in the same buffer. This can be explained by the fact that the estimations used require that the particle is spherical and the solution homogeneous, this is not the case for phage. In addition, for QELS measurements, rotational diffusion should be taken into account, and the real value of R_H will be somewhat greater. Nevertheless, one can see from the light-scattering measurements that the phage dimensions increase substantially with lowering the ionic strength.

All of the methods applied gave some characteristic data on the phage as a whole and on its DNA stability, but no information about its structural organization could be obtained. In order to investigate the inner structure, phage samples in the two buffers were

studied by SAXS. This method has already been applied to T7 in buffer H. A very precise scattering curve over a wide angular range was obtained, several geometrical and weight parameters of the phage were determined. The model of its shape was proposed (Rontó et al. 1983), and the map of electron density in an axially-symmetric approximation was reconstructed by a direct method (Svergun et al. 1982).

Both samples in buffers H and L were measured in the same angular region and under the same conditions. The desmeared scattering curves are presented in Fig. 3 (it should be noted that the curve for the H buffer coincides well with the curve obtained earlier (Rontó et al. 1983)). Qualitative considerations show that the behaviour of the curves is quite similar in the beginning (until $s = 0.2\,\mathrm{nm}^{-1}$). Both of them show a distinct maximum at $s = 2.6\,\mathrm{nm}^{-1}$, which corresponds to Bragg spacing 2.4 nm (the so-called DNA packing maximum). At the same time, the behaviour of the two curves in the region $0.2 < s < 2.5\,\mathrm{nm}^{-1}$ is different, though a large number of subsidiary maxima in both curves indicates high monodispersity of the samples.

Some integral parameters of the phage in buffers H and L were calculated from these curves. The radii of gyration as evaluated by Guinier approximation prove to be 28.5 nm for the buffer H and 25.3 nm for L. The particle volumes estimated by the Porod invariant resulted in the values of $1.14 \times 10^5\,\mathrm{nm}^3$ and $9.1 \times 10^4\,\mathrm{nm}^3$ respectively.

It was also possible to calculate the radii of gyration of the phage head ($R_{S(\mathrm{head})}$) from the positions of initial subsidiary maxima (Rontó et al. 1983). These values proved to be 23.6 and 24.8 nm, respectively.

Note that these data are in apparent contradiction to the above listed ones since the phage dimensions in buffer L are according to SAXS nearly the same (or even less) than in buffer H. Apart from this, the head radius coincides with the radius of the whole particle in buffer L, being 10% smaller in buffer H.

To get more information on the phage structure, distance distribution functions ($p(r)$) for the two cases were calculated (Fig. 4). In both cases they were calculated for independent experimental runs. The functions for these runs coincide within the accuracy as plotting in Fig. 4 (see vertical bar in figure). One can see the curves coincide well up to the diameter of 60 nm which corresponds to the region of the phage head ($R = 30$ nm). At the same time, for $r > 60$ nm the $p(r)$ curve for the buffer H sample decreases gradually because of the influence of the phage tail, while the curve for buffer L drops almost to zero at $r = 62$ nm followed by the maximum at $r = 76$ nm.

Since the phage head is isometric and the tail is sufficiently small (about 4% of the particle volume) the spherically-symmetric approximation is applicable. The calculated radial electron density distributions in

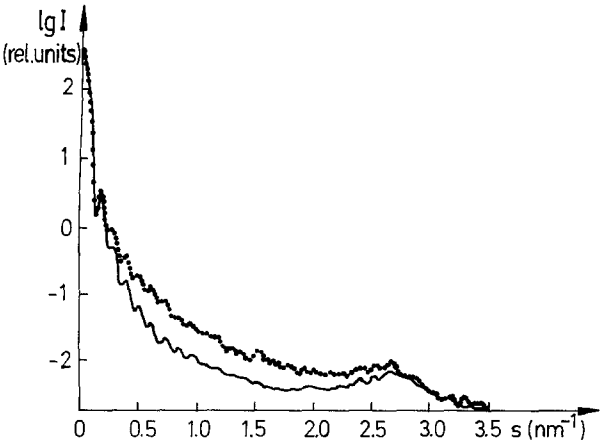

Fig. 3. Small-angle X-ray scattering curves of phage T7 measured in buffers H (——) and L (....)

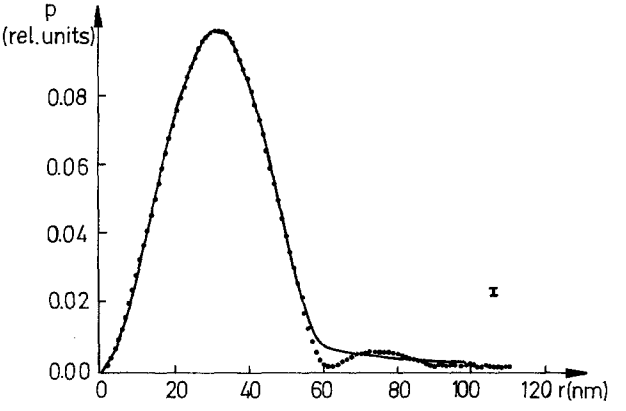

Fig. 4. Distance distribution of the electron density of phage T7 calculated in the cases of buffers H (——) and L (....). The vertical bar indicates the maximum deviation for both curves obtained for different runs

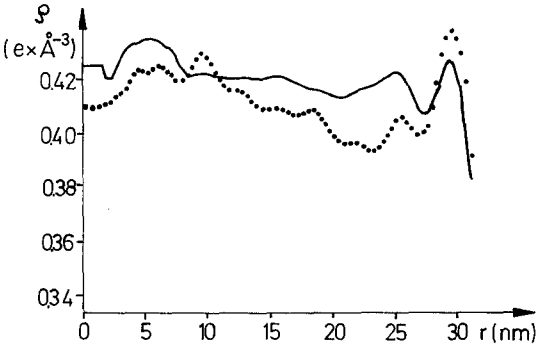

Fig. 5. Radial electron density distribution of phage T7 calculated in the cases of buffers H (——) and L (....)

absolute units are shown in Fig. 5. Here one can neglect the differences of these functions at very small r ($r < 7$ nm) since the integral transformation is unstable in this range; the ripples in the curves are caused by termination effects. One can see that the behaviour of the two curves also differs in the higher r range: the

radial density for buffer H is nearly constant, while for buffer L it decreases gradually.

Based on the SAXS data the following model of structural changes can be proposed. In the L buffer a portion of peripheral intraphage DNA moves through the capsid out of the phage head forming some "shell" of DNA spread around the head (Fig. 6). The observed decrease of radial DNA density at the outer part of the phage head is therefore taken into account; the behaviour of the $p(r)$ function is readily explained by considering 76 nm as an average diameter of the shell. At the same time the R_g value will be practically the same (or can even decrease) since outer parts of the DNA spread would be "invisible" for X-rays because of negligibly small excess electron density (such "loss" of DNA could, in principle, diminish the forward X-ray scattering, however the accuracy of absolute measurements is not sufficient to judge this). The phage tail could be either disrupted or masked by the shell, therefore the "head" radius of gyration would coincide with the particle one.

The model agrees well with the results of other observations. Really, QELS and viscosity measurements will "see" all the volume moving together with the particle, while SLS data will correspond to the volume occupied by the phage itself and by the organized solvent as well. In all these cases the whole volume occupied by DNA spreads will be seen and the apparent phage dimensions would increase substantially.

The higher AMT binding ability of the phage in buffer L can be explained not only through the higher binding capacity of DNA in respect to the charged drug at the low ion concentration, but also by the higher accessibility of the phage DNA. Inactivation of phage T 7 in this buffer can be caused, from one side by DNA masking the places on the phage surface which serve as the attachment for the host bacteria or by some steric inhibition of injection. The role of some possible DNA damage can not be excluded on the basis of our presented results.

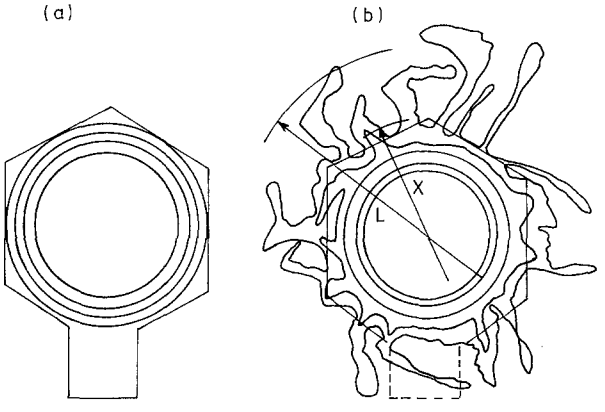

Fig. 6 a and b. Schematic views of DNA packaging for buffer H (**a**) and L (**b**). Here X denotes average dimension of the DNA outer shell as seen by X-rays; L corresponds to phage dimension as determined by light scattering and viscosity measurements

Conclusion

The parallel application of different structure- and function-investigation methods made it possible to propose a model explaining the structural reasons for phage inactivation in low ionic strength buffers. Phages undergo conformational changes concerning the higher order structure and the stability of the intraphage DNA which partly comes out of the protein capsid, resulting in modifications of the surface and of the hydrodynamic behaviour of the phage. The higher drug-accessibility which must be taken into account in pharmacological investigations can also be explained.

References

Ausio J, Borochov N, Seger D, Eisenberg H (1984) Interaction of chromatin with NaCl and $MgCl_2$. J Mol Biol 177:373–398

Cummings HZ, Pike ER (1974) Photon correlation and light beating spectroscopy. Plenum Press, New York

Fekete A, Rontó GY, Feigin LA, Tikhonychev VV, Módos K (1982) Temperature dependent structural changes of intraphage T 7 DNA. Biophys Struct Mech 9:1–9

Gáspár S, Módos K, Rontó GY (1980) Complex method for the determination of the physiological parameters of bacteriumphages systems. In: Fedina L, Kanyár B, Kollai M (eds) Adv Physiol Sci n34: Mathematical and computational methods in physiology. Pergamon Press – Akadémiai Kiadó, Budapest, pp 141–146

Glatter O, Kratky O (1982) Small-angle X-ray scattering. Academic Press, London, p 525

Kerker M (1969) The scattering of light and other electromagnetic radiation. Academic Press, New York, pp 432–433

Larcom LL, Dodds EC, McNeil WF (1981) Effect of cation concentration on sensitivity of DNA to UV inactivation. Photobiochem Photobiophys 2:181–186

Lohman TM, De Haseth PL, Record Jr Mt (1978) Analysis of ion concentration effects on the kinetics of protein-nucleic acid interactions. Biophys Chem 8:261–294

Mogilevski LYu, Dembo AT, Svergun DI, Feigin LA (1984) Small-angle scattering diffractometer with position sensitive detector. Kristallografia (in russian) 29:587–591

Rolbin YuA, Svergun DI, Schedrin BM (1980) On the flattening of small-angle scattering curves. (Engl transl) Sov Phys Crystallogr 25 (2):133–137

Rontó GY (1984) Biological macromolecules and liquid crystals. Acta Biochim Biophys Acad Sci Hung 19(3–4):221–228

Rontó GY, Agamalyan MM, Drabkin GM, Feigin LA, Lvov YuM (1983) Structure of bacteriophage T7 (Small-angle X-ray and neutron scattering study). Biophys J 43(3):309–314

Schedrin BN, Feigin LA (1966) Slit-height collimation correction for finite slits in small-angle scattering. (Engl transl) Sov Phys Crystallogr 11 (2):166–168

Schellman JA, Parthasarathy N (1984) X-ray diffraction studies on cation-collapsed DNA. J Mol Biol 175:313–329

Serwer PH (1976) Internal proteins of bacteriophage T7. J Mol Biol 107:271–291
Svergun DI, Feigin LA, Schedrin BM (1982) Small-angle scattering: Direct structure analysis. Acta Crystallogr A38: 827–835
Svergun DI, Feigin LA, Schedrin BM (1984) The solution of one dimensional sign problem for Fourier transform. Acta Crystallogr A40:137–142
Strauss JH, Sinsheimer RL (1963) Purification and properties of bacteriophage MS2 and of its ribonucleic acids. J Mol Biol 7:43–48
Studier FW (1972) Bacteriophage T7. Science 174:367–376
Studier FW, Moffatt BA (1986) Bacteriophage T7 RNA polymerase to direct selective high-level expression of cloned genes. J Mol Biol 189:113–130
Tóth K, Rontó GY (1987) Salt-effects on the bacteriophage T7 – I. Physiol Chem Phys Med NMR 19:59–66
Tóth K, Csik G, Rontó GY (1987) Salt-effects on the bacteriophage T7 – II. Physiol Chem Phys Med NMR 19:67–74